Al-Khwarizmi Engineering Journal

Al-Khwarizmi Engineering Journal
ISSN (printed): 1818 – 1171, ISSN (online): 2312 – 0789
Vol. 21, No. 3, September, (2025), pp. 66- 75

Studying the Effect of Rotor's Coefficients on a Y-shaped Tri-copter

Abdullah Mohammed Yahia[1]*, Ahmed Alkamchi[2] and Ergun Erçelebi[3]

[1,2] *Department of Mechatronics, Al-Khwarizmi College of Engineering, University of Baghdad, Baghdad, Iraq*
[3] *Electrical and Electronic Department, College of Engineering, Gaziantep University, Turkey*
*Corresponding Author's Email: abd.yahia2102m@kecbu.uobaghdad.iq

(Received 23 May 2024; Revised 21 October 2024; Accepted 28 December 2024; Published 1 September 2025)
https://doi.org/10.22153/kej.2025.12.002

Abstract

Unmanned aerial vehicles (UAVs) are small yet highly capable aircraft widely used in many applications. UAV designs and shapes vary depending on their intended usage. Tri-copters, known for their agility, have three propellers. However, one of their main challenges is yawing, which occurs when the UAV rotates around its z-axis (yaw angle). This yawing issue is a result of the asymmetry in the number of propellers. Unlike quadcopters, which have an even number of propellers, the aerodynamic drag torque produced by the tri-copter's propellers' does not cancel out. In this paper, a Y-shaped tri-copter model is tested, modified and compared to address the yawing problem. Aiming to mitigate yawing, two propellers are set to rotate clockwise, whilst the third propeller rotates clockwise. In the first configuration, the force coefficient is set equally for all propellers. In the second configuration, the force coefficient of the counter-clockwise rotating propeller is doubled. The UAV model is controlled by six PIDs associated with feedback linearisation for both configurations—three PIDs for attitude control and three for altitude control. The PIDs are tuned using a genetic algorithm, and the system is simulated in MATLAB Simulink. The proposed configuration demonstrates lower integral time absolute error (ITAE) values, indicating improved UAV performance. The average ITAE values for the Y-shaped model are 0.1553 for the first case and 0.1017 for the second case. The second case shows remarkable tracking in the desired output, with no violation of design limitations (servo angles and motor speeds).

Keywords: *PID; genetic algorithm; UAV; thrust-vectoring; feedback-linearisation.*

1. Introduction

Unmanned aerial vehicles (UAVs) are small aircraft that can be controlled remotely or by an onboard navigation unit. UAVs have a wide range of applications across various fields, leading to numerous configurations (including bi-copters, tri-copters and quad-copters), each with different frame shapes and motor configurations [1]. Bi-copters are amongst the simplest in terms of the number of actuators. They typically have only two to four actuators: two main propellers and one or two additional servo motors to control yaw and roll motions[2, 3]. The control systems of bi-copters are considered challenging due to the limited number of actuators, making them under-actuated. Thus, bi-copters are governed by a set of non-linear equations and generally offer less stability [4]. Quad-copters are amongst the most reliable UAVs, utilising four propellers (under-actuated)[5]. By adding two to four servo motors, these UAVs can be fully actuated[6] or even over actuated[7], simplifying control. However, one of the main challenges for UAVs is power consumption, which can limit their capabilities and flight time [8]. In contrast, tri-copters are known for their power efficiency because they use only three rotors [9]. Aiming to enhance agility and manoeuvrability [10], a thrust-vectoring mechanism can be added. The main issue with tri-copters is yawing, which

arises from the asymmetry in rotor numbers and their rotational directions. With three rotors, the aerodynamic forces acting on the blades of each rotor do not cancel out, leading to yaw instability. This issue can be addressed by using coaxial rotors [11], implementing specific control strategies[12] or employing tiltable rotors[13]. Tilt mechanisms can be integrated into different configurations to meet desired application demands, as shown in [14], [15] and [16]. For system control, various methods have been verified; for example, the linear quadratic regulator is used in [17], H-infinity is used in [18] and a proportional integral derivative (PID) is applied in [19]. The PID control, when associated with optimisation techniques to maximise system performance, can be a very practical approach to UAV control [20]. Various optimisation techniques, such as grey wolf optimisation, have been employed for this purpose [21].

2. Y Tri-coper Mathematical Model

In this section, the mathematical model of the UAV is presented for two different motor configurations (two cases). The UAV parameters are referenced from [22], as shown in Table 1.

Table 1,
UAV parameters

parameter	Description	Value
m	UAV Mass	1.448 kg
a	Arm length	0.33 m
I_{xx}	Body inertia of x axis	0.1035 $kg.m^2$
I_{yy}	Body inertia of y axis	0.1003 $kg.m^2$
I_{zz}	Body inertia of z axis	0.1709 $kg.m^2$
k_f	Force coefficient	1.084 × 10−5 $kg.m$
k_t	Torque coefficient	1.726 × 10−7 $kg.m^2$

The primary model and dynamic equations are sourced from [23], along with the feedback linearisation equation, incorporating a modification to the original motor rotation directions. In both cases, the motor rotation directions are consistent: the front motors rotate clockwise, whilst the rear motor rotates counter-clockwise, as shown in Figure 1. In this context, α represents the servo angle, with the subscripts referring to the corresponding arm (right [r], left [l] and back [l]), and 'a' denotes the arm length, which is equal for all arms.

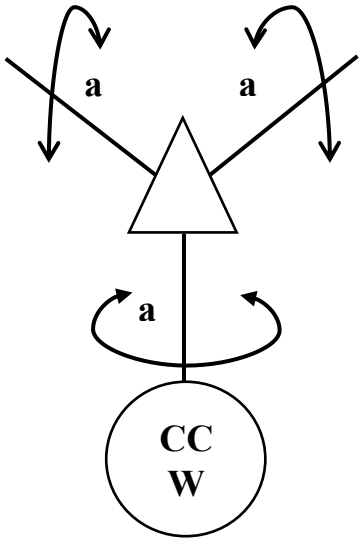

Fig. 1. UAV motor configuration

The motor coefficients will only differ in the second case, where the back motor coefficients are doubled. When this modification is implemented, certain adjustments to the original model will be required, as shown below.

2.1. First Case

In this case, the force coefficient for all motors will remain the same. The only change will be the direction of the rear motor, which will affect the mathematical representation of the drag torque, as shown below:

$$\tau_{d1} = \begin{bmatrix} 0.866k_t\omega_{m_r}^2 cos(\alpha_r) - 0.866k_t\omega_{m_l}^2 sin(\alpha_l) \\ -k_t\omega_{m_r}^2 sin(\alpha_r) + 0.5k_t\omega_{m_l}^2 sin(\alpha_l) - 0.5k_t\omega_{m_b}^2 sin(\alpha_b) \\ -k_t\omega_{m_r}^2 cos(\alpha_r) - k_t\omega_{m_l}^2 cos(\alpha_l) + k_t\omega_{m_b}^2 cos(\alpha_b) \end{bmatrix} \quad \ldots(1)$$

where $\tau_{d()}$ is the drag torque for the corresponding case, k_t is the torque coefficient, $\alpha_{()}$ is the servo angle for the corresponding arm (b for back, r for right and l for left) and $\omega_{()}^2$ is the squared angular velocity for the corresponding arm.

2.1. Second Case

In this case, the drag torque will remain the same as in case one because the motor's rotation directions are set identically. The only difference is that the torque coefficient for the back motor is doubled.

$$\tau_{d2} = \begin{bmatrix} 0.866k_t\omega_{m_r}^2 cos(\alpha_r) - 0.866k_t\omega_{m_l}^2 sin(\alpha_l) \\ -k_t\omega_{m_r}^2 sin(\alpha_r) + 0.5k_t\omega_{m_l}^2 sin(\alpha_l) + 2(-0.5k_t)\omega_{m_b}^2 sin(\alpha_b) \\ -k_t\omega_{m_r}^2 cos(\alpha_r) - k_t\omega_{m_l}^2 cos(\alpha_l) + 2k_t\omega_{m_b}^2 cos(\alpha_b) \end{bmatrix} \quad \ldots(2)$$

By doubling the force coefficient, the force and torque equations are modified as shown below:

$$f = \begin{bmatrix} -0.866k_f\omega_{m_l}^2 sin(\alpha_l) + 0.866(2k_f)\omega_{m_b}^2 sin(\alpha_b) \\ k_f\omega_{m_r}^2 sin(\alpha_r) + -0.5k_f\omega_{m_l}^2 sin(\alpha_l) + 2(-0.5k_f)\omega_{m_b}^2 sin(\alpha_b) \\ k_f\omega_{m_r}^2 cos(\alpha_r) + k_f\omega_{m_l}^2 cos(\alpha_l) + 2k_f\omega_{m_b}^2 cos(\alpha_b) \end{bmatrix} \quad \ldots(3)$$

$$\tau = \begin{bmatrix} 0.866k_f\omega_{m_l}^2 cos(\alpha_l) - 0.866(2k_f)\omega_{m_b}^2 cos(\alpha_b) \\ -k_f\omega_{m_r}^2 cos(\alpha_r) + 0.5k_f\omega_{m_l}^2 cos(\alpha_l) + 2(0.5k_f)\omega_{m_b}^2 cos(\alpha_b) \\ k_f\omega_{m_r}^2 sin(\alpha_r) + k_f\omega_{m_l}^2 sin(\alpha_l) + 2k_f\omega_{m_b}^2 sin(\alpha_b) \end{bmatrix} \quad \ldots(4)$$

where k_f is the force coefficient, f is the total force and τ is the total torque.

3. Proposed Controller

The tri-rotor equations exhibit strong output coupling, necessitating the use of PID controllers in combination with feedback linearisation. As referenced in Section 1, the feedback linearisation method is also adopted from previous work. A total of six PID controllers are used to control the UAV: three for position control (x, y, z) and three for attitude control (ϕ, θ, ψ). This control approach remains the same for both cases, as shown in Figure 2.

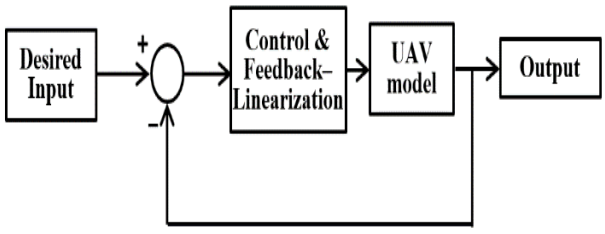

Fig. 2. System block diagram

3.1 Proportional Integral Divertive Controller (PID)

After linearising the system, a linear PID controller can be applied. The PID controller is considered an optimal choice due to its simple implementation and high efficiency [24]. The standard PID formula used to compute the error signal is referenced from [25].

$$u(t) = K_P e(t) + K_I \int e(t)dt + K_D \dot{e}(t) \quad \ldots(5)$$

where K_P is the proportional gain, K_I is the integral gain, K_D is the derivation gain and $e(t)$ represents the error signal. The system uses six PID controllers, divided between position and attitude control. Each controller is separately tuned using the genetic algorithm (GA) optimisation method, with the integral time absolute error (ITAE) used as the cost function.

3.2 PID Tunning

The PIDs are tuned using the GA, a method introduced by John Holland in 1975 [26]. Based on the concepts of evolution, GA operate by choosing the most adapted individuals (elite members) form a population to reproduce and generate a new generation. This process involves selecting individuals, evaluating their performance, combining their solutions through genetic crossover, applying random mutations and modifying the population with the best-performing solutions. This approach, which mirrors the concept of natural selection, is effective for minimising specific cost functions (in this case, the system error). The GA is used to tune the PID controllers for both cases, implemented using a built-in MATLAB function. The selected cost function for evaluating performance is the ITAE [27].

$$\int_0^\infty t|e(t)|dt \quad \ldots(6)$$

Figure 3 shows the genetic algorithm flow chart.

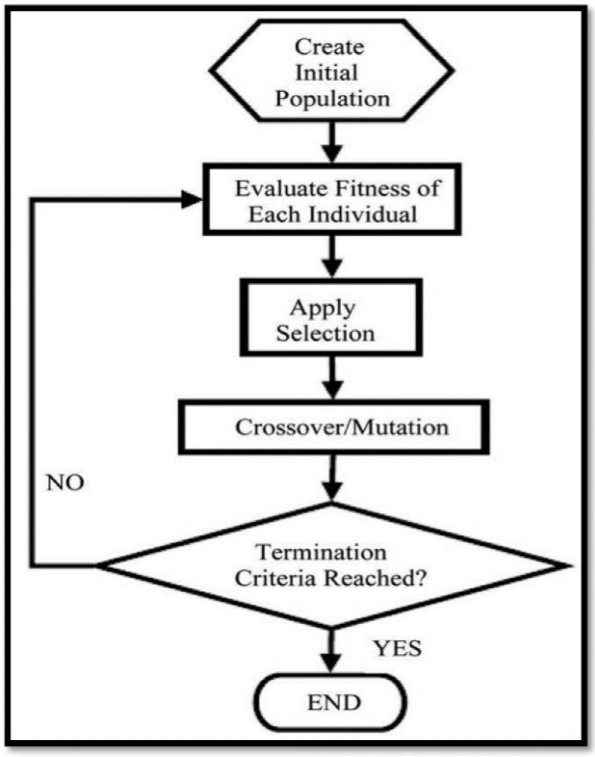

Fig. 3. Genetic algorithm working steps flow chart [28]

4. Simulation Results

The PID parameters are tuned by setting the desired outputs for position and altitude to 1 m and 10deg for attitude. In this section, the system responses for both cases will be represented, along with their corresponding ITEA values and a simulated flight scenario. Each case will be evaluated based on its tracking performance and control efficiency.

4.1. First Case

The PID gain and the ITAE values for the first case are shown in Table 2.

Table 2
PID parameters, first case

parameter	kp	ki	kd	ITEA
Phi	14.64	0.397	3.63	0.0421
Theta	19.48	0.033	4.15	0.0241
Psi	19.77	0.03	4.72	0.0252
x	18.58	16.06	4.21	0.3591
y	19.85	14.49	4.02	0.3605
z	17.9	0.026	4.58	0.1211

Figures 4 and 5 show the tuning responses for the altitude and attitude, respectively, during the tuning process for the first case. The performance metrics of case one are as follows: altitude settle time: (1.7 s), X overshoot: (38%), Y overshoot: (37%) and Z overshoot: (10%). For case one, attitude settle time is (2.1 s), Phi overshoot is 17%, Theta overshoot is 16 % and Psi overshoot is 11%.

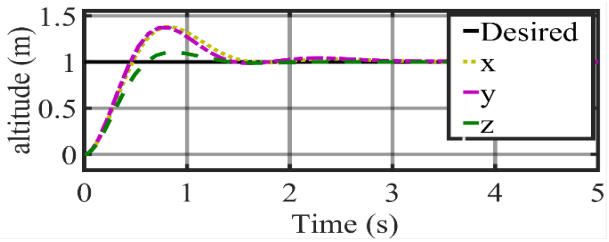

Fig. 4. UAV altitude response for the first case

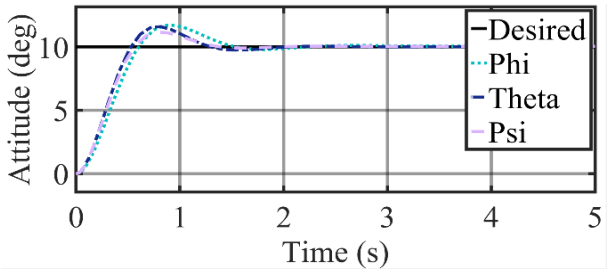

Fig. 5. UAV attitude response for the first case

4.2. Second Case

The second case showed lower ITAE values after doubling the back motor's coefficients, as shown in Table 3.

Table 3
PID parameters, second case

parameter	kp	ki	kd	ITEA
Phi	19.98	0.595	4.97	0.0307
Theta	19.26	0.015	5.67	0.0167
Psi	19.63	0.403	3.7	0.0368
x	19.82	0.018	5.83	0.0889
y	18.57	18.03	4.45	0.3447
z	19.81	0.016	5.46	0.0924

Figures 6 and 7 illustrate the tuning responses for altitude and attitude, respectively, during the tuning process of the second case. The performance metrics of case two are as follows: altitude settle time: (1.7 s), X overshoot: (3%), Y overshoot: (40%) and Z overshoot: (5%). For Case two, attitude

settle time is 2 s, Phi overshoot is 10%), Theta overshoot is 11% and Psi overshoot is 22%.

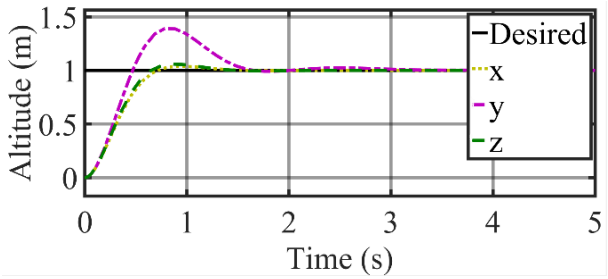

Fig. 6. UAV altitude response for the first case

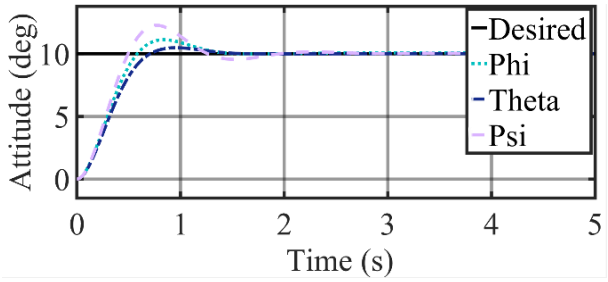

Fig. 7. UAV attitude response for the first case

The second case demonstrated lower ITAE values; thus, a flight scenario was then applied to further evaluate the UAV performance. The UAV is initially positioned at (0,1,0), ascending vertically and then follows a spiral shape. This approach is achieved using a circular equation for the x and y coordinates, a ramp function for the z coordinate and setting all attitude variables to zero. Figure 8 illustrates the flight scenario.

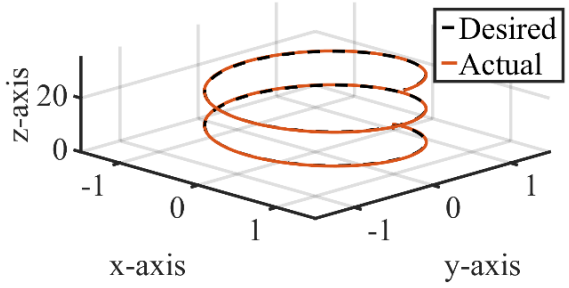

Fig. 8. UAV helical flight scenario

The UAV smoothly tracked due to its enhanced manoeuvrability provided by the thrust vectoring mechanism. The motor forces remained balance due to the back motor having increased force and torque coefficients. Aiming to thoroughly evaluate the system's performance, the responses of altitude, attitude, motor speeds and servo angles were captured during the flight. Figure 9 shows the altitude response.

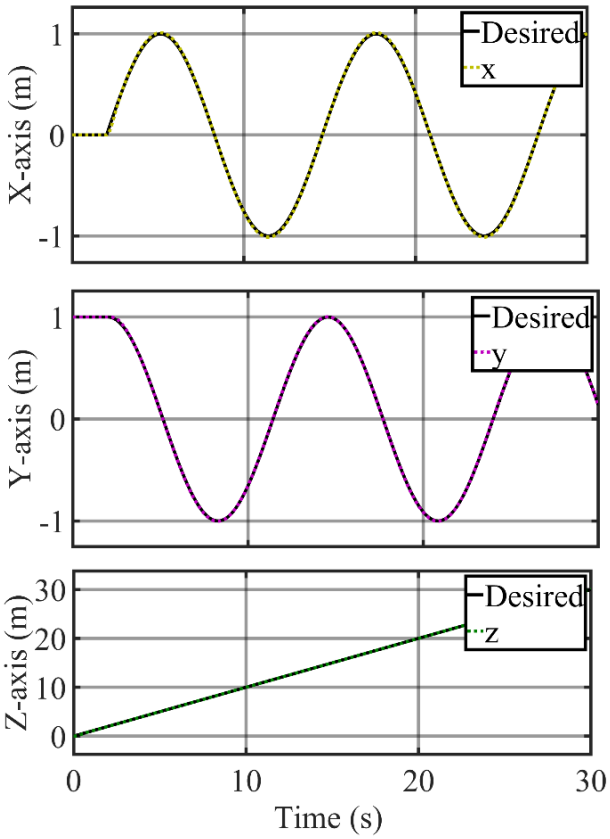

Fig. 9. UAV helical flight scenario altitude response

The altitude responses closely followed the desired trajectory without any issues, demonstrating the UAV's effective manoeuvrability. Figure 10 displays the attitude response.

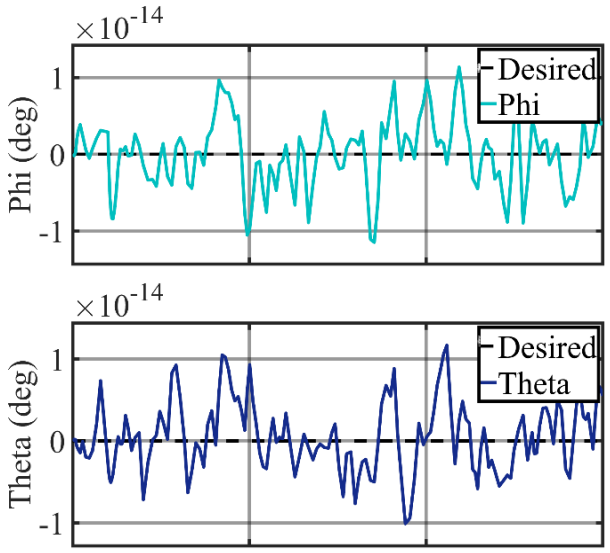

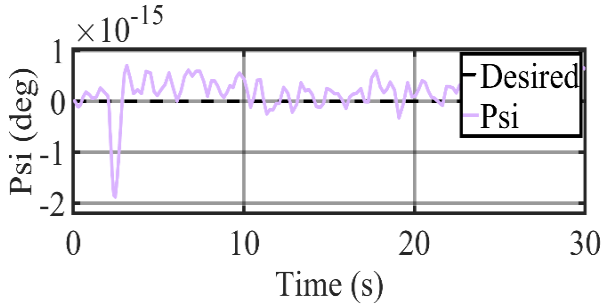

Fig. 10. UAV helical flight scenario attitude response

The attitude responses remained zero throughout the entire flight, indicating that the UAV maintained good balance. Figures 11 and 12 show the responses of the motors and servo motors, respectively. The motor speed limits are set between 0 and 3600 rpm, whilst the servo angle limits range from −90° to 90°.

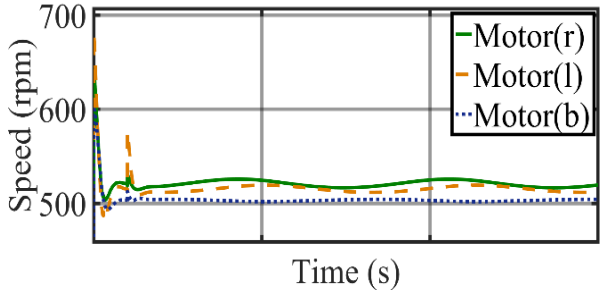

Fig. 11. UAV helical flight scenario motors response

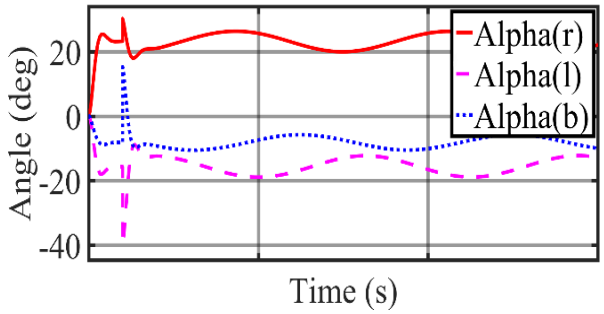

Fig. 12. UAV helical flight scenario servo motors response

The motors speed values increased as the UAV took off, then settled at a specific value and did not exceed the design boundaries. The back motor shows lower speed values because it has larger coefficients. The responses of the servo angles change continuously to maintain the UAV on the desired path. The second case showed lower ITAE values; therefore, a disturbance test and an uncertainty test were then applied to further evaluate the UAV's performance. The uncertainty test responses and ITAE values after changing the mass to 1.8 kg and the arm length to 0.2 m are shown in Table 4.

Table 4
Uncertainty ITAE values, second case

Parameter	ITEA uncertainty
Phi	0.03
Theta	0.016
Psi	0.035
x	0.09
y	0.347
z	0.093

Figure 13 shows the uncertainty test responses for altitude and attitude. All responses stabilise within approximately 2 s.

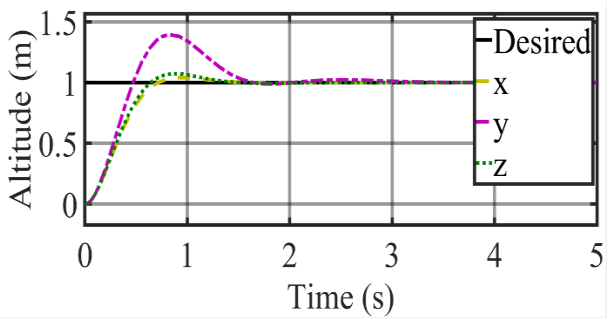

(a)

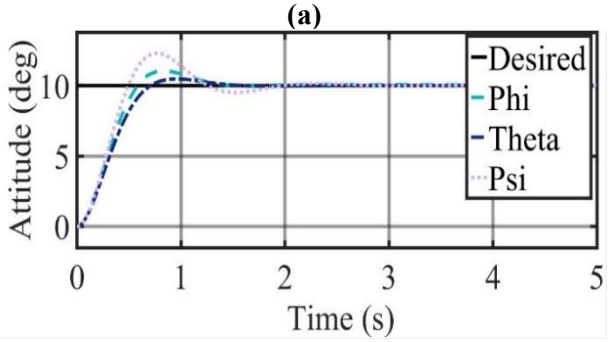

(b)

Fig. 13. Uncertainty altitude & attitude responses for Y-Model: (a) Altitude responses, (b) Attitude responses

Figure 14 shows an impulse disturbance applied along the z-axis. The disturbance has a magnitude of 5 N and lasts for 0.25 s, starting at T = 4 s. The system regains stability approximately 1 s after the disturbance ends.

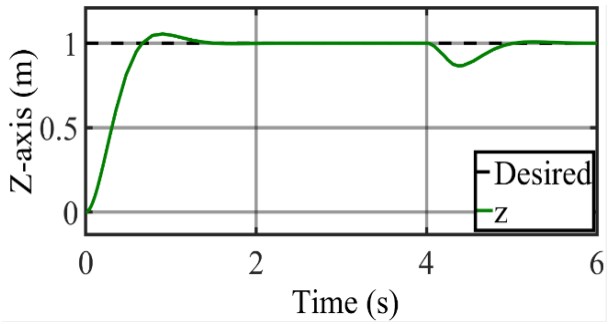

Fig. 14. Disturbance on z axis

Figure 15 shows disturbances on the phi rotation angle. The disturbance has a magnitude of 10 N.m. This disturbance starts at T = 2.5 s and ends at T = 2.75 s. The system regains stability approximately 2 s after the disturbance ends.

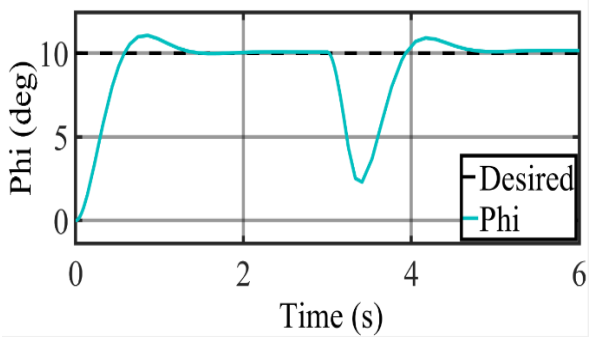

Fig. 15. Disturbance on phi

5. Conclusion

This research aims to study the effects of rotor coefficients on UAV performance. A previously developed model is modified by changing the rotation direction of the rotors: the front two propellers are set to rotate clockwise, and the back propeller rotates counter-clockwise. The modified model is then divided into two cases. Case one includes the model with the changed rotation direction and no further modifications, whilst case two involves doubling the coefficients of the back motor. Both cases are linearised using feedback linearisation to address the output coupling problem and are controlled by six PID controllers. The PID controllers are tuned using a GA, with the ITAE as the cost function. The average ITAE values for the Y-shaped model are 0.1553 and 0.1017 for cases one and two, respectively. Case two showed improved tracking of the desired output in the applied scenario without exceeding design limitations (servo angles and motor speeds). Aiming to further investigate the effects of rotor coefficients, implementation on a model without thrust vectoring is recommended.

Notations

x	x- axis, m
y	y- axis, m
z	z- axis, m
f	Force, N
a	Length, m
k_f	Force coefficient, $N.s^2$
k_t	Torque coefficient, $N.m.s^2$
m	Mass, kg
I_{xx}	Body inertia of x-axis, $kg.m^2$
I_{yy}	Body inertia of y-axis, $kg.m^2$
I_{zz}	Body inertia, of z-axis $kg.m^2$
e	Error
K_p	Proportional PID gain
K_i	integral PID gain
K_d	Derivative PID gain

Greek symbols

α	Servo angle, deg
ϕ	Roll angle, deg
θ	Pitch angle, deg
ψ	Yaw angle, deg
τ	Torque, $N.m$
ω	Angular velocity, rpm

References

[1] M. H. Sabour, P. Jafary, and S. Nematiyan, "Applications and classifications of unmanned aerial vehicles: A literature review with focus on multi-rotors," The Aeronautical Journal, vol. 127, no. 1309, pp. 466–490, 2023, doi: 10.1017/aer.2022.75.

[2] Y. Qin, N. Chen, Y. Cai, W. Xu, and F. Zhang, "Gemini II: Design, Modeling, and Control of a Compact Yet Efficient Servoless Bi-copter," IEEE/ASME Transactions on Mechatronics, vol. 27, no. 6, pp. 4304–4315, Dec. 2022, doi: 10.1109/TMECH.2022.3153587.

[3] Q. Zhang, Z. Liu, J. Zhao, and S. Zhang, "Modeling and attitude control of Bi-copter," AUS 2016 - 2016 IEEE/CSAA International Conference on Aircraft Utility Systems, pp. 172–176, Nov. 2016, doi: 10.1109/AUS.2016.7748042.

[4] K. Fufa Advisor, P. Alluvada Co-Advisor, and A. Thetlar, "Design controller stability of bi-copter unmanned aerial vehicle at hovering position," 2019, Accessed: Jun. 04, 2024. [Online]. Available: https://repository.ju.edu.et//handle/123456789/5535

[5] Ø. Magnussen and K. E. Skjønhaug, "Modeling, design and experimental study for a quadcopter system construction," 95, [10], 2011, Accessed: Jun. 04, 2024. [Online]. Available: https://uia.brage.unit.no/uia-xmlui/handle/11250/136686

[6] M. Nigro, F. Pierri, and F. Caccavale, "Preliminary design, modeling and control of a fully actuated quadrotor UAV," in 2019 International Conference on Unmanned Aircraft Systems (ICUAS), IEEE, Jun. 2019, pp. 1108–1116. doi: 10.1109/ICUAS.2019.8798092.

[7] M. Ryll, H. H. Bülthoff, and P. R. Giordano, "A novel overactuated quadrotor unmanned aerial vehicle: Modeling, control, and experimental validation," IEEE Transactions on Control Systems Technology, vol. 23, no. 2, pp. 540–556, Mar. 2015. doi: 10.1109/TCST.2014.2330999.

[8] P. Beigi, M. S. Rajabi, and S. Aghakhani, "An Overview of Drone Energy Consumption Factors and Models," Handbook of Smart Energy Systems, pp. 529–548, 2023. doi: 10.1007/978-3-030-97940-9_200.

[9] S. Salazar-Cruz, R. Lozano, and J. Escareño, "Stabilization and nonlinear control for a novel trirotor mini-aircraft," Control Eng Pract, vol. 17, no. 8, pp. 886–894, 2009 https://doi.org/10.1016/j.conengprac.2009.02.013.

[10] R. Siswoyo Jo, A. E. G. Tan, M. Tee Kit Tsun, and H. Siswoyo Jo, "Design and Modeling of Actuation System of Unmanned Tricopter with Thrust-Vectoring Front Tilt Rotors for Sustainable Flying," Lecture Notes in Mechanical Engineering, pp. 45–55, 2020. doi: 10.1007/978-981-15-4756-0_5.

[11] A. D. H. Arroyo, A. S. Morais, G. V. Lima, and L. Ribeiro, "Modeling and Simulation of a Novel Tilt-Wing-Coaxial-Rotor Tricopter," Simpósio Brasileiro de Automação Inteligente - SBAI, vol. 1, no. 1, Oct. 2021. doi: 10.20906/SBAI.V1I1.2627.

[12] B. H. Sababha, H. M. Al Zu', N. A. bi, and O. A. Rawashdeh, "A rotor-tilt-free tricopter UAV: design, modelling, and stability control," International Journal of Mechatronics and Automation, vol. 5, no. 2/3, p. 107, 2015. doi: 10.1504/IJMA.2015.075956.

[13] S. M. M. Rahman, M. Mashud, and M. Assad-Uz-Zaman, "Design and implementation of a Y-copter: Aerobatic version," AIP Conf Proc, vol. 1851, no. 1, Jun. 2017. doi: 10.1063/1.4984718/885537.

[14] M. S. Atif, Z. Haider, M. M. Zohaib, and M. A. Raza, "Embedded and Control Systems Design and Implementation of T-Shaped Tilt-Rotor Tri-copter," 2021 7th International Conference on Control Science and Systems Engineering, ICCSSE 2021, pp. 78–82, Jul. 2021. doi: 10.1109/ICCSSE52761.2021.9545147.

[15] A. W. Summers, "Modeling and Control of a Fixed Wing Tilt-Rotor Tri-Copter," 2017, Accessed: May 03, 2024. [Online]. Available: https://digital.lib.washington.edu:443/researchworks/handle/1773/39911

[16] M. Umer, S. M. A. Kazmi, S. M. H. Askari, and I. A. Rana, "Design and Modeling of VTOL Tri Tilt-rotor Aircraft," 2018 15th International Conference on Smart Cities: Improving Quality of Life Using ICT and IoT, HONET-ICT 2018, pp. 127–131, Nov. 2018. doi: 10.1109/HONET.2018.8551474.

[17] A. Houari, I. Bachir, D. K. Mohame, and M. K. Mohamed, "PID vs LQR controller for tilt rotor airplane," International Journal of Electrical and Computer Engineering (IJECE), vol. 10, no. 6, p. 6309, Dec. 2020. doi: 10.11591/ijece.v10i6.pp6309-6318.

[18] M. K. Mohamed and A. Lanzon, "Design and control of novel tri-rotor UAV," in Proceedings of the 2012 UKACC International Conference on Control, CONTROL 2012, 2012, pp. 304–309. doi: 10.1109/CONTROL.2012.6334647.

[19] A. Cadena, R. Ponguillo, and D. Ochoa, "Development of Guidance, Navigation and Control System Using FPGA Technology for an UAV Tricopter," Lecture Notes in Mechanical Engineering, pp. 363–375, 2017. doi: 10.1007/978-3-319-33581-0_28.

[20] Y. Li, K. H. Ang, and G. C. Y. Chong, "PID Control System Analysis and Design: Problems, Remedies, and Future Directions," IEEE Control Syst, vol. 26, no. 1, pp. 32–41, 2006. doi: 10.1109/MCS.2006.1580152.

[21] S. J. Raheema and M. H. Saleh, "An Experimental Research on Design and Development Diversified Controllers for Tri-copter Stability Comparison," IOP Conf Ser

Mater Sci Eng, vol. 1105, no. 1, p. 012019, Jun. 2021, doi: 10.1088/1757-899X/1105/1/012019.

[22] "Modelling, Control and Construction of Tricopter Unmanned Aerial Vehicles — Research Explorer the University of Manchester." Accessed: May 07, 2024. [Online]. Available: https://research.manchester.ac.uk/en/studentTheses/modelling-control-and-construction-of-tricopter-unmanned-aerial-v

[23] M. K. Mohamed and A. Lanzon, "Design and control of novel tri-rotor UAV," in Proceedings of the 2012 UKACC International Conference on Control, CONTROL 2012, 2012, pp. 304–309. doi: 10.1109/CONTROL.2012.6334647.

[24] A. Alkamachi and E. Ercelebi, "MODELLING AND CONTROL OF H-SHAPED RACING QUADCOPTER WITH TILTING PROPELLERS," Facta Universitatis, Series: Mechanical Engineering, vol. 15, no. 2, pp. 201–215, Aug. 2017, doi: 10.22190/FUME170203005A.

[25] A. K. J., "PID Controllers: Theory, Design, and Tuning," The International Society of Measurement and Control, 1995, doi: 10.11499/SICEJL1962.40.679.

[26] B. H. Sumida, A. I. Houston, J. M. McNamara, and W. D. Hamilton, "Genetic algorithms and evolution," J Theor Biol, vol. 147, no. 1, pp. 59–84, Nov. 1990, doi: 10.1016/S0022-5193(05)80252-8.

[27] A. H. Yousif Yacoub, S. Buyamin, and N. Abdul Wahab, "Integral Time Absolute Error Minimization For Pi Controller On Coupled–Tank Liquid Level Control System Based On Stochastic Search Echniques," J Teknol, Mar. 2012, doi: 10.11113/jt.v54.823.

[28] A. Hassanat, K. Almohammadi, E. Alkafaween, E. Abunawas, A. Hammouri, and V. B. S. Prasath, "Choosing Mutation and Crossover Ratios for Genetic Algorithms—A Review with a New Dynamic Approach," Information, vol. 10, no. 12, p. 390, Dec. 2019, doi: 10.3390/info10120390.

دراسة تأثير معاملات الدوار على مروحية ثلاثية الشكل على شكل حرفY

عبد الله محمد يحيى[1]* احمد محروس راغب*[2] اركون ارچلبي[3]

[1،2] قسم هندسة الميكاترونكس، كلية الهندسة الخوارزمي، جامعة بغداد، بغداد، العراق
[3] قسم الهندسة الكهربائية والالكترونية، جامعة غازي عنتاب، تركيا
*البريد الالكتروني: abd.yahia2102m@kecbu.uobaghdad.edu.iq

المستخلص

الطائرات بدون طيار هي طائرات صغيرة ولكنها قادرة على العمل بكفاءة وتستخدم على نطاق واسع في العديد من التطبيقات. هناك العديد من التصاميم والأشكال للطائرات بدون طيار اعتمادًا على استخدامها. تعد الطائرات ثلاثية المراوح واحدة من أكثر الطائرات بدون طيار رشاقة؛ لأنها تحتوي على ثلاثة مراوح فقط. ومع ذلك، فإن إحدى مشاكلها هي انعراج الطائرة بدون طيار وهو دوران الطائرة بدون طيار حول محورها z (زاوية الانعراج). يحدث ذلك بسبب عدم التماثل في أعداد المراوح. بمعنى آخر، لن يتم إلغاء عزم السحب الناتج عن الديناميكا الهوائية لشفرات المراوح كما هو الحال في طائرة رباعية المراوح (عدد زوجي من المراوح). في هذه العمل تم اختبار نموذج طائرة ثلاثية المراوح على شكل حرف Y وتعديله ومقارنته؛ لتقليل تأثير مشكلة الانعراج، ويتم ضبط مروحتين في اتجاه عقارب الساعة، بينما يتم ضبط المروحة الثالثة في الاتجاه المعاكس. يتم ضبط معامل القوة بالتساوي لجميع المراوح في الحالة الأولى. ثم يتم مضاعفة معامل القوة للمروحة الواحدة التي تدور في اتجاه عكس اتجاه عقارب الساعة للحالة الثانية. فيتم التحكم في النموذج من خلال ستة معرّفات PID مرتبطة بالخطية الراجعة لكلا التكوينين ثلاثة للموقف، وثلاثة للارتفاع. يتم ضبط معرّفات PID باستخدام خوارزمية وراثية ويتم محاكاة النظام في MATLAB Simulink. يظهر التكوين المقترح قيم ITAE أقل (خطأ مطلق زمني متكامل) مما يشير إلى أداء أفضل للطائرات بدون طيار. متوسط قيم ITAE للنموذج على شكل Y هو (٠,١٥٥٣) للحالة الأولى، و (٠,١٠١٧) للحالة الثانية. أظهرت الحالة الثانية تتبعًا كبيرًا للإخراج المطلوب في السيناريو المطبق ولم تتجاوز قيود التصميم (زوايا المؤازرة وسرعات المحركات).